

Towards disentangling the contributions of articulation and acoustics in multimodal phoneme recognition

Sean Foley^{1,2}, Hong Nguyen¹, Jihwan Lee¹, Sudarsana Reddy Kadiri¹, Dani Byrd², Louis Goldstein², Shrikanth Narayanan¹

¹Signal Analysis and Interpretation Laboratory, University of Southern California, USA

²Department of Linguistics, University of Southern California, USA

seanfole@usc.edu

Abstract

Although many previous studies have carried out multimodal learning with real-time MRI data that captures the audio-visual kinematics of the vocal tract during speech, these studies have been limited by their reliance on multi-speaker corpora. This prevents such models from learning a detailed relationship between acoustics and articulation due to considerable cross-speaker variability. In this study, we develop unimodal audio and video models as well as multimodal models for phoneme recognition using a long-form single-speaker MRI corpus, with the goal of disentangling and interpreting the contributions of each modality. Audio and multimodal models show similar performance on different phonetic manner classes but diverge on places of articulation. Interpretation of the models' latent space shows similar encoding of the phonetic space across audio and multimodal models, while the models' attention weights highlight differences in acoustic and articulatory timing for certain phonemes.

Index Terms: phoneme recognition, multimodal models, speech production, real-time MRI

1. Introduction

Speech is inherently multimodal, with the integration of sensory and motor information being essential to both speech production and perception [1, 2, 3]. In speech production, individual variability in both articulation and its consequent acoustics is robust [4, 5]. A crucial aspect of this variability concerns the realization of targets, even within the long-standing debates as to whether the targets of speech production are acoustic or articulatory or a combination of both [6, 7, 8]. In continuous speech, achieving a target can be framed as the successful encoding of phonological information, particularly the identity of the phonemes being spoken (in contrast to others). The recognition of phonemes is then a problem of multimodal learning, with the possibility that, for a given phoneme, one modality may be more informative than the other or that both are flexibly integrated at short and/or longer timescales in perception.

In multimodal machine learning, audio-visual models often use video that captures the movements of the jaw, face and lips [9, 10], a view typical of a listener in everyday conversation. The focus of the current study is multimodal learning using speech data captured using real-time MRI (rtMRI), which typically captures simultaneous video of the soft-tissue vocal tract (generally in mid-sagittal orientation) covering the entire airway from lips to the larynx and speech audio [11, 12]. Such video allows for capturing the kinematics of the tongue, jaw, lips, velum, and larynx, i.e. the major articulators employed in speech production. This permits models to be better-aligned with the causal mechanisms underlying speech production.

A number of previous studies have used such speech data in a variety of speech classification tasks [13, 14, 15, 16, 17]. [13] used solely rtMRI video of the vocal tract to classify different vowel-consonant-vowel (VCV) sequences using a combination of RNNs and CNNs. [15] used both video and audio to perform phone classification and recognition on the USC-TIMIT corpus [18], finding that multimodal information resulted in better performance than either unimodal case. Both [14] and [16] used the USC Vocal Tract Morphology corpus [19] for phone classification and VCV classification respectively, with the former using a CNN-based approach and the latter a Transformer-based model. With the USC 75-Speaker Dataset [12], [17] related self-supervised model performance in phoneme recognition to cross-speaker differences in articulation, as illuminated in MRI video.

While previous studies have conducted multimodal speech classification using rtMRI audio and video, few have specifically attempted to disentangle the contribution of each modality in the given task. Typically, differences in some metric across unimodal audio/video only and multimodal models are used to assess the benefit of multimodal information [15, 16]. Crucially, this method primarily serves to distinguish model performance but does not offer a robust measure of the information gain provided by each modality, particularly in the identification of individual phonemes. Additionally, all previous studies have relied on multimodal data from multiple speakers. This limits the model's ability to learn a concise and veridical relationship between acoustics and articulation, given the considerable cross-speaker variability in articulation and vocal tract morphology [4, 20].

The current study aims to disentangle the role of acoustics and articulation in the task of phoneme recognition from continuous speech, with a particular focus on the benefits gained by adding articulatory information in comparison to using audio features alone. The study makes use of a long-form single speaker rtMRI corpus, allowing the models to learn a robust relationship between acoustic and articulatory information. The results highlight similarities and differences in the performance of audio-only and multimodal models in identifying phonemes of certain phonetic classes. Additionally, the current study develops tactics for interpreting both the latent space and the attention weights of such models. As such, this study provides one of the more thorough interpretations of multimodality in phoneme recognition.

2. Method

2.1. Model

The primary module for the model architecture is a Conformer, following the design in [21], which consists of two feed-forward

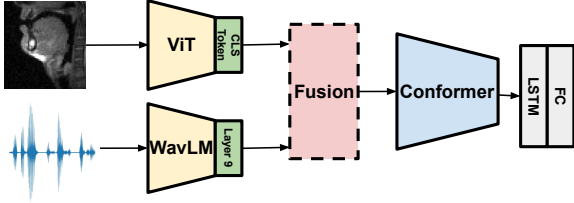


Figure 1: *Model architecture for the current study.*

modules, a self-attention layer, and a convolution module (see [21] for further details), accessed via TorchAudio. The output of the Conformer is decoded by a single LSTM layer, with a final linear layer used for prediction. In the unimodal cases, the input to the Conformer consists of either acoustic features $\mathbf{A} \in \mathbb{R}^{t \times D}$ or video features $\mathbf{V} \in \mathbb{R}^{t \times D}$, where t is the temporal dimension and D is the feature dimension. For the multimodal model, the audio and video features are concatenated along the temporal dimension, such that $\mathbf{M} \in \mathbb{R}^{t \times 2D}$. For the task of phoneme recognition, the model is trained using the connectionist temporal classification (CTC) loss [22]. As a baseline, we performed zero-shot phoneme recognition on the audio using Wav2Vec2Phoneme, accessed via Hugging Face [23].

2.2. Analysis

Overall phoneme recognition is calculated using Phoneme Error Rate (PER). Additionally, PER for individual phonemes is calculated using the edit distance for sequences containing the target phoneme and dividing by the number of occurrences of that phoneme in the ground truth sequence. These values were averaged across manner and place of articulation classes. To get a sense of how acoustic, video, or multimodal features may capture the phonetic space differently, the latent representations from the Conformer convolution module were extracted for individual phonemes by slicing them in the temporal dimension using the ground truth time-stamps and then averaging across the temporal dimension.

Following [16], the attention weights from the self-attention layer of the last Conformer layer were extracted. While [16] considered the effects of adding audio features to the attention weights in comparison to using only video features, we investigate the opposite effect, specifically the effect of adding video features compared to using only audio features. This tactic stems from the possibility that differences in articulatory and acoustic timing may be evident for certain phonemes. The attention weights were averaged across the attention heads, and then for each key the average query value was calculated, which provides values for the degree to which each time step is attended to by the entire sequence. Phoneme time stamps were used to get phoneme-level attention values, with 25 ms windows on either side to capture potential coarticulatory effects. All attention weights were z -scored after averaging across the attention heads.

3. Experiments

3.1. Dataset

We use a new single speaker rtMRI corpus with simultaneously recorded audio and video. The corpus contains speech data from one male native speaker of American English producing the 460 sentences used in the USC TIMIT corpus, passages used

in the USC 75-Speaker Dataset [12] and spontaneous speech prompted on topics such as food, hobbies, travel, etc. The vocal tract of the speaker was imaged in midsagittal orientation using a 0.55T MRI scanner with a custom upper airway receiver coil [24], resulting in a frame rate of 99 frames/sec [25]. Audio was collected at 16 kHz. In total, approximately one hour of audio data was collected, comparable to the MNGU0 EMA corpus [26]. First-pass phoneme alignments were extracted using the Montreal Forced Aligner (MFA) and manually corrected by a phonetician in Praat.

3.2. Pre-processing

Audio: From the raw audio, speech segments were extracted using the pre-trained Voice Activity Detection (VAD) model pyannote, accessed via Hugging Face. The resulting VAD speech segments were concatenated or split into chunks of up to 5 sec in length. Word boundaries were used to split speech segments longer than 5 sec. Both the audio and video were chunked using these time intervals, resulting in 767 chunks, for a total duration of 38 min and an average duration of 2.95 sec per chunk. These chunks were split into train/test sets with a ratio of 0.7/0.3. The audio chunks were first denoised using the denoiser model in [27], and then features were extracted from the 9th layer of the pre-trained base WavLM model [28], based on previous work demonstrating that this layer encodes rich phonetic information [29].

Video: The original MRI video was cropped to focus on the vocal tract region, with the upper hard palate, larynx, and pharyngeal wall serving as boundaries (see Figure 1). All video frames were rescaled to a spatial resolution of 224×224 . For each frame, we took the classification (CLS) token from the last hidden layer of the base ViT model [30], which was fine-tuned on MRI video from 10 native American English speakers in the USC 75-Speaker Dataset [12] using a self-supervised approach [31, 32]. Linear interpolation was used to match the sampling rate of the audio and video features, with the audio features being upsampled.

3.3. Implementation details

The Conformer model was initialized with the same general configuration described in [21]. The input dimension to the Conformer was set to 768 for the unimodal models and 2×768 for the multimodal model, with a feed-forward dimension of 256. The number of attention heads was set at 4, a kernel size of 31, and dropout set at 0.3. The number of Conformer layers was set to 3. For the LSTM layer, the latent size was 128, which served as the input size for the final linear layer. For all models, the Adam optimizer was used, with a batch size of 8 and a learning rate of $1e-3$, which was decayed by a factor of 0.9 every 20 epochs. Learning rate, batch size, and weight decay were set using a grid search over the range of [$1e-3$, $5e-4$, $1e-4$], [8, 16, 32], and [$1e-3$, $5e-4$, $1e-4$] respectively. All models were trained on an NVIDIA A40 GPU.

4. Results

4.1. Phoneme error rate (PER)

The overall PER results on the held-out test set are presented in Table 1. The results reported here are from the best performing model on the test set, based on the CTC loss. The baseline Wav2Vec2Phoneme model achieved a zero-shot PER of 0.36. While no previous study has performed phoneme recognition

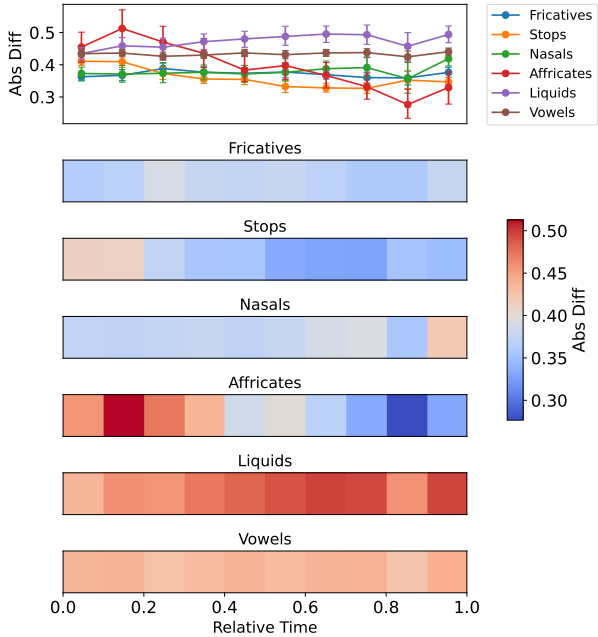


Figure 4: Absolute difference in attention weights at each time step between audio and multimodal models per phoneme manner class.

to-fricative transition of these segments.

An example highlighting the timing differences across the modalities is shown in Figure 5 for the phrase “a roll”. Notice that there is quite a discrepancy between the two models during the /ə/, /ɹ/, and /oʊ/ intervals. The bottom panel shows the MRI video frames during /ə/ and /ɹ/. The multimodal model attends more to the onset of the /ə/ interval and more towards the end of the /ɹ/ interval, with clear unattended regions after these times. The audio model attends more to the center of /ə/ and overall much more to the /oʊ/ sequence. The MRI frames show clearly that the tongue tip constriction for /ɹ/ starts to form *before* the acoustic onset of /ə/, while the /oʊ/ constriction is formed during the /ɹ/ offset. While the audio model attention aligns more with the formant structure, the multimodal model attention is highly localized to intervals containing crucial constriction information.

5. Discussion

In this study, we trained unimodal audio and video models and a combined multimodal model on phoneme recognition using a long-form single-speaker rtMRI corpus. The PER results showed that our audio model significantly outperforms the baseline model and those from similar previous work, which attests to the robustness of the WavLM representations in learning phonetic information. As expected, the unimodal video model does not perform as well as the audio model, given that acoustic features generally outperform the more sparse visual speech information in speech recognition tasks. The multimodal model performs only slightly worse than the audio model, suggesting overall that adding the video features does not improve performance.

At the level of specific phoneme classes, the unimodal audio and video models performed similarly, in that they performed best on nasals and liquids and did not perform as well on

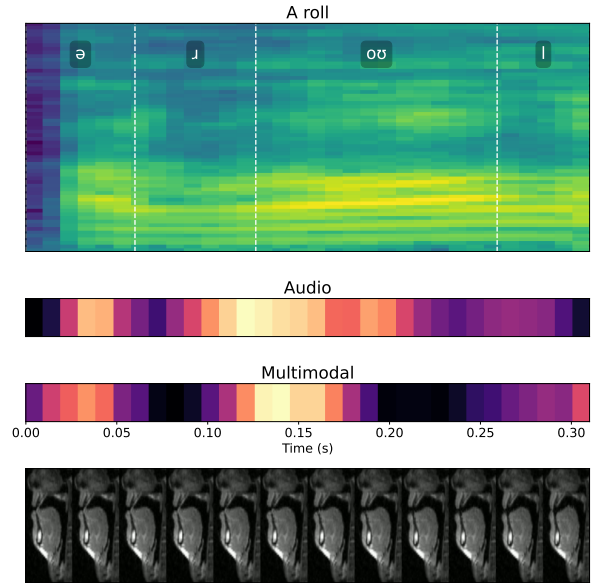


Figure 5: Log-mel spectrogram (top) and audio and multimodal attention weights (middle) for the phrase “a roll”, with MRI frames for the phonemes /ə/ and /ɹ/ (bottom). Lighter attentions have higher values.

affricates and stops. This is unsurprising as nasals and liquids both have distinctive acoustic and articulatory characteristics, such as anti-resonance structure, multiple constrictions, and for rhotics a low third formant [34, 35]. Capturing the sequential stop-to-fricative transition that distinguishes stops and affricates is likely challenging for both audio and video modalities.

Interpretation of the models’ latent spaces aligns with the phoneme-level PER performance in that more well-formed clusters were found for sibilants, nasals, and liquids, while stops and labio-dental fricatives show more local overlap in their clusters. Interestingly, despite all models performing best on liquids, vowels, and nasals, the models’ attention weights differed most between the audio and multimodal models for liquids and vowels. This suggests that the addition of video features can actually force the model to attend to different information. Coarticulation in the articulatory domain is robust and may not always have a clear acoustic correlate. As shown in Figure 5, it appears likely that phoneme-relevant information is available *earlier* when articulatory information is present and that the multimodal model relies more on this information than the acoustic-only model.

Despite the progress made here in interpreting multimodality in phoneme recognition, there are a number of limitations to the current study. First, while the corpus used here has more single-speaker MRI data than is available in public datasets, the total speech time after applying VAD was only 38 minutes. Such limited data undoubtedly still limits the ability of the model to learn strong connections between acoustics and articulation. Second, the current study only implemented this approach with an off-the-shelf Conformer architecture, and replicating this work with other architectures for the task of phoneme recognition could offer further insights into the sort of information gained by the incorporation of audio and video (articulation) modalities for this task.

6. Acknowledgments

This work was supported by NIH grant T32 DC009975.

7. References

- [1] G. Hickok, J. Houde, and F. Rong, "Sensorimotor integration in speech processing: computational basis and neural organization," *Neuron*, vol. 69, no. 3, pp. 407–422, 2011.
- [2] J. H. Venezia, P. Fillmore, W. Matchin, A. L. Isenberg, G. Hickok, and J. Fridriksson, "Perception drives production across sensory modalities: A network for sensorimotor integration of visual speech," *NeuroImage*, vol. 126, pp. 196–207, 2016.
- [3] L. Goldstein, "The role of temporal modulation in sensorimotor interaction," *Frontiers in Psychology*, vol. 10, p. 2608, 2019.
- [4] D. H. Whalen, W.-R. Chen, M. K. Tiede, and H. Nam, "Variability of articulator positions and formants across nine english vowels," *Journal of phonetics*, vol. 68, pp. 1–14, 2018.
- [5] S. K. Harper, *Individual differences in phonetic variability and phonological representation*. University of Southern California, 2021.
- [6] C. P. Browman and L. Goldstein, "Articulatory phonology: An overview," *Phonetica*, vol. 49, no. 3-4, pp. 155–180, 1992.
- [7] G. Hickok, "The architecture of speech production and the role of the phoneme in speech processing," *Language, Cognition and Neuroscience*, vol. 29, no. 1, pp. 2–20, 2014.
- [8] M. D. Faytak, *Articulatory uniformity through articulatory reuse: insights from an ultrasound study of Sūzhōu Chinese*. University of California, Berkeley, 2018.
- [9] B. Shi, W.-N. Hsu, K. Lakhotia, and A. Mohamed, "Learning audio-visual speech representation by masked multimodal cluster prediction," *arXiv preprint arXiv:2201.02184*, 2022.
- [10] Y. Wu, Y. Peng, Y. Lu, X. Chang, R. Song, and S. Watanabe, "Robust audiovisual speech recognition models with mixture-of-experts," *arXiv preprint arXiv:2409.12370*, 2024.
- [11] Y. Lim, P. Kumar, and K. S. Nayak, "Speech production real-time mri at 0.55 t," *Magnetic Resonance in Medicine*, vol. 91, no. 1, pp. 337–343, 2024.
- [12] Y. Lim, A. Toutios, Y. Bliesener, Y. Tian, S. G. Lingala, C. Vaz, T. Sorensen, M. Oh, S. Harper, W. Chen *et al.*, "A multispeaker dataset of raw and reconstructed speech production real-time mri video and 3d volumetric images," *Scientific data*, vol. 8, no. 1, p. 187, 2021.
- [13] P. Saha, P. Srungarapu, and S. Fels, "Towards automatic speech identification from vocal tract shape dynamics in real-time mri," *arXiv preprint arXiv:1807.11089*, 2018.
- [14] K. Van Leeuwen, P. Bos, S. Trebeschi, M. J. van Alphen, L. Voskuilen, L. E. Smeele, F. van der Heijden, R. van Son *et al.*, "Cnn-based phoneme classifier from vocal tract mri learns embedding consistent with articulatory topology," in *Interspeech*, 2019, pp. 909–913.
- [15] Ö. D. Köse and M. Saraçlar, "Multimodal representations for synchronized speech and real-time mri video processing," *IEEE/ACM Transactions on Audio, Speech, and Language Processing*, vol. 29, pp. 1912–1924, 2021.
- [16] Y. Yue, M. Proctor, L. Zhou, R. Gupta, T. Piyadasa, A. Gully, K. Ballard, and C. Jin, "Towards speech classification from acoustic and vocal tract data in real-time mri," in *Proceedings of INTER-SPEECH 2024*, 2024.
- [17] X. Shi, T. Feng, K. Huang, S. R. Kadiri, J. Lee, Y. Lu, Y. Zhang, L. Goldstein, and S. Narayanan, "Direct articulatory observation reveals phoneme recognition performance characteristics of a self-supervised speech model," *JASA Express Letters*, vol. 4, no. 11, 2024.
- [18] S. Narayanan, A. Toutios, V. Ramanarayanan, A. Lammert, J. Kim, S. Lee, K. Nayak, Y.-C. Kim, Y. Zhu, L. Goldstein *et al.*, "Usc-timit: A database of multimodal speech production data," USC, Tech. Rep., 2013.[Online] <http://sail.usc.edu/span/usc-timit...>, Tech. Rep., 2013.
- [19] T. Sorensen, Z. I. Skordilis, A. Toutios, Y.-C. Kim, Y. Zhu, J. Kim, A. C. Lammert, V. Ramanarayanan, L. Goldstein, D. Byrd *et al.*, "Database of volumetric and real-time vocal tract mri for speech science," in *Interspeech*, 2017, pp. 645–649.
- [20] A. Serrurier, P. Badin, L. Lamalle, and C. Neuschaefer-Rube, "Characterization of inter-speaker articulatory variability: A two-level multi-speaker modelling approach based on mri data," *The Journal of the Acoustical Society of America*, vol. 145, no. 4, pp. 2149–2170, 2019.
- [21] A. Gulati, J. Qin, C.-C. Chiu, N. Parmar, Y. Zhang, J. Yu, W. Han, S. Wang, Z. Zhang, Y. Wu *et al.*, "Conformer: Convolution-augmented transformer for speech recognition," *arXiv preprint arXiv:2005.08100*, 2020.
- [22] A. Graves, S. Fernández, F. Gomez, and J. Schmidhuber, "Connectionist temporal classification: labelling unsegmented sequence data with recurrent neural networks," in *Proceedings of the 23rd International Conference on Machine Learning*, ser. ICML '06. New York, NY, USA: Association for Computing Machinery, 2006, p. 369–376. [Online]. Available: <https://doi.org/10.1145/1143844.1143891>
- [23] Q. Xu, A. Baevski, and M. Auli, "Simple and effective zero-shot cross-lingual phoneme recognition," *arXiv preprint arXiv:2109.11680*, 2021.
- [24] F. Muñoz, Y. Lim, S. X. Cui, H. Stark, and K. S. Nayak, "Evaluation of a novel 8-channel rx coil for speech production mri at 0.55 t," *Magnetic Resonance Materials in Physics, Biology and Medicine*, vol. 36, no. 3, pp. 419–426, 2023.
- [25] P. Kumar, Y. Tian, Y. Lim, S. X. Cui, C. Hagedorn, D. Byrd, U. K. Sinha, S. Narayanan, and K. S. Nayak, "State-of-the-art speech production mri protocol for new 0.55 tesla scanners," in *Interspeech 2024*, 2024, pp. 2590–2594.
- [26] K. Richmond, P. Hoole, and S. King, "Announcing the electromagnetic articulography (day 1) subset of the mngu0 articulatory corpus," in *Twelfth Annual Conference of the International Speech Communication Association*, 2011.
- [27] A. Defossez, G. Synnaeve, and Y. Adi, "Real time speech enhancement in the waveform domain," *arXiv preprint arXiv:2006.12847*, 2020.
- [28] S. Chen, C. Wang, Z. Chen, Y. Wu, S. Liu, Z. Chen, J. Li, N. Kanda, T. Yoshioka, X. Xiao *et al.*, "Wavlm: Large-scale self-supervised pre-training for full stack speech processing," *IEEE Journal of Selected Topics in Signal Processing*, vol. 16, no. 6, pp. 1505–1518, 2022.
- [29] C. J. Cho, P. Wu, A. Mohamed, and G. K. Anumanchipalli, "Evidence of vocal tract articulation in self-supervised learning of speech," *arXiv preprint arXiv:2210.11723*, 2022.
- [30] D. Alexey, "An image is worth 16x16 words: Transformers for image recognition at scale," *arXiv preprint arXiv: 2010.11929*, 2020.
- [31] T. Chen, S. Kornblith, M. Norouzi, and G. Hinton, "A simple framework for contrastive learning of visual representations," *arXiv preprint arXiv:2002.05709*, 2020.
- [32] S. Azizi, L. Culp, J. Freyberg, B. Mustafa, S. Baur, S. Kornblith, T. Chen, P. MacWilliams, S. S. Mahdavi, E. Wulczyn *et al.*, "Robust and efficient medical imaging with self-supervision," *arXiv preprint arXiv:2205.09723*, 2022.
- [33] L. Van der Maaten and G. Hinton, "Visualizing data using t-sne," *Journal of machine learning research*, vol. 9, no. 11, 2008.
- [34] A. Alwan, S. Narayanan, and K. Haker, "Toward articulatory-acoustic models for liquid approximants based on mri and epg data. part ii. the rhotics," *The Journal of the Acoustical Society of America*, vol. 101, no. 2, pp. 1078–1089, 1997.
- [35] M. Proctor, R. Walker, C. Smith, T. Szalay, L. Goldstein, and S. Narayanan, "Articulatory characterization of english liquid-final rimes," *Journal of Phonetics*, vol. 77, p. 100921, 2019.